Jurnal Teknologi

Full Paper

DETECTION OF FRACTURED AQUIFER USING COMBINATION OF RESISTIVITY AND INDUCED POLARIZATION ANALYSIS

Mohamed Azwan Mohamed Zawawi, Noorellimia Mat Toridi*, Aimrun Wayayok

Dept of Biological and Agricultural Engineering, Faculty of Engineering, Universiti Putra Malaysia, Malaysia

Article history
Received
15 July 2015
Received in revised form
2 August 2015
Accepted
26 August 2015

*Corresponding author
noorellimia1@gmail.com

Graphical abstract

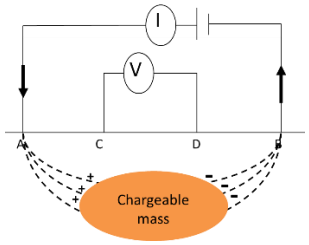

Abstract

Subsurface geological formation is essential in investigating the groundwater occurrence. The formation can be determined from subsurface resistivity value through electrical survey. However, there is ambiguity in interpreting the subsurface resistivity. Therefore the purpose of this study is to delineate the subsurface geological formation through combination of resistivity and induced polarization analysis. The type of geological formation is determined from resistivity analysis and well lithology. Meanwhile the fracture, water in clayey soil and groundwater occurrence is identified through combination of resistivity and induced polarization analysis. It has been identified that the study areas consist of fractured aquifer. Possible groundwater fractured area can be indicated by low resistivity ranged from 700 to 2000 Ωm and overlapped with low chargeability ranged from 1 msec to 2 msec. This study provides useful information on nature of groundwater occurrence especially fractured aquifer.

Keywords: Electrical resistivity, induced polarization, fractured aquifer

1.0 INTRODUCTION

Electrical survey is conducted to determine the subsurface resistivity distribution. The subsurface resistivity is related to the geological formation by comparing the resistivity value to well lithology. Electrical survey can be done either through 1D resistivity sounding or 2D resistivity survey. In 1D resistivity sounding, the center point of electrode array remains fixed. The spacing between electrodes is increased to get deeper sections of the subsurface. An advantage of this method is, it gives discrete lateral changes in subsurface resistivity (Loke, 2000). The subsurface geological formation may vary laterally and horizontally. Thus it is essential to identify the lateral and horizontal changes in the subsurface resistivity. 2D electrical resistivity is the practical solutions to delineate the subsurface resistivity. However there is ambiguity in interpreting the subsurface resistivity. Low resistivity can either indicate higher clay content or higher water content. Induced polarization analysis may be able to reduce the ambiguity (Dahlin *et al*., 2002). The purpose of this study is to delineate the subsurface geological formation by using combination of resistivity and induced polarization analysis.

2.0 GEOELECTRICAL THEORIES

2.1 Resistivity measurement

In 2D electrical resistivity survey, a current is introduced into the ground through electric current electrodes (A,B). The potential field is measured using two electrodes (C,D) as in Figure 1 below.

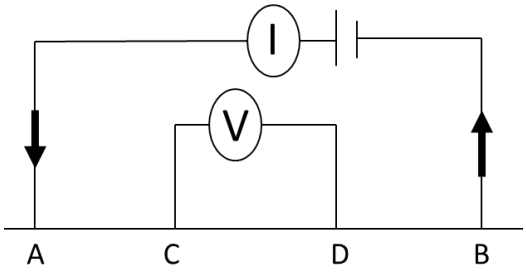

Figure 1 Electrode configuration

From the electric current (I) and the potential difference (V) value, an apparent resistivity value is calculated using the Ohm's law as follows:

$$V_r = I\rho_a \quad (1)$$

Considering a point source and homogeneous earth, the potential field must have cylindrical symmetry with respect to the vertical line through the current source as shown in Figure 2 below.

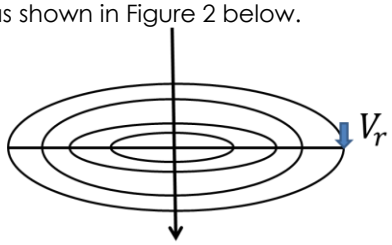

Figure 2 Potential field of cylindrical symmetry

The potential at a point in the distance r is calculated as follows:-

$$V_r = \frac{\rho_a I}{2\pi r} \quad (2)$$

Thus the potential at electrode point C (V_C) is calculated as follows:-

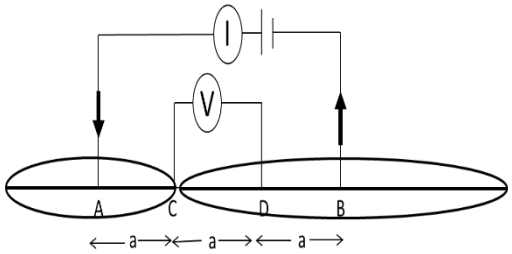

Figure 3 Voltage measured at potential electrode C

The electric current (I) flow from high potential to low potential. Thus, V_C at distance AC is higher than V_C at distance CB.

$$V_c = \frac{\rho_a I}{2\pi AC} - \frac{\rho_a I}{2\pi CB} \quad (3)$$

$$V_c = \frac{\rho_a I}{2\pi}\left(\frac{1}{AC} - \frac{1}{CB}\right) \quad (4)$$

Same concept applies to the voltage measured at potential electrode D.

$$V_D = \frac{\rho_a I}{2\pi}\left(\frac{1}{AD} - \frac{1}{BD}\right) \quad (5)$$

The potential difference between C and D is as follows:-

$$\mathrm{V} = V_c - V_D \quad (6)$$

$$\mathrm{V} = \frac{\rho_a I}{2\pi}\left[\left(\frac{1}{AC} - \frac{1}{CB}\right) - \left(\frac{1}{AD} - \frac{1}{BD}\right)\right] \quad (7)$$

$$\rho_a = \frac{2\pi V}{I}\left[\frac{1}{\left(\frac{1}{AC} - \frac{1}{CB} - \frac{1}{AD} + \frac{1}{BD}\right)}\right] \quad (8)$$

The equation is simplified with geometric factor (k)

$$\rho_a = \frac{V}{I}k \quad (9)$$

Where

$$k = 2\pi\left[\frac{1}{\left(\frac{1}{AC} - \frac{1}{CB} - \frac{1}{AD} + \frac{1}{BD}\right)}\right] \quad (10)$$

k is dependent on array. For example k in Wenner array is given as in Figure 3.

$$k_{wenner} = 2\pi a \quad (11)$$

k for Schlumberger is given as follows where distance between AB = L, CD = a and AC = DB ≠ CD :-

$$k_{schlumberger} = \pi\left(\frac{L^2 - a^2}{a}\right) \quad (12)$$

Details of theories on electrical resistivity measurement is explained by Anomohanran (2015). The measured apparent resistivity is presented in term of pseudosection. The measured apparent resistivity is a function of true layer resistivity, their boundaries, and the location of the electrodes (Asfahani, 2007). As apparent resistivity is influenced by the geometry of electrode (Loke, 1995), the apparent resistivity do not represent the actual subsurface (Boucher *et al.*, 2009). The general function for apparent resistivity can be written as in equation 13.

$$\rho_a = f\left(\begin{matrix}true\ layer\ resistivity,\\ their\ boundaries, location\ of\ electrodes\end{matrix}\right) \quad (13)$$

The measured apparent resistivity is the dependent variable or the output. True layer resistivity is the independent variable or parameter. In order to estimate the parameter from output, inversion is needed. In this study, inversion have been done through a computer program, RES2DINV (Loke, 2000).

The parameter which is the true layer resistivity is estimated through approximation method. Using the approximated parameter, the apparent resistivity is calculated. This process is done iteratively until an acceptable fit between measured and calculated apparent resistivity is achieved (Boucher *et al*., 2009; Griffiths & Barker, 1993).

2.2 Induced Polarization Measurement

Induced polarization is conducted to reduce ambiguity such as distinguish between groundwater and clay soil.

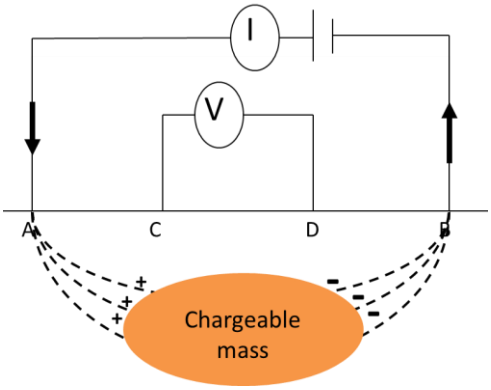

Figure 4 Induced polarization measurement

As electric current flow through the mass, the positive charges will pile up at outer side of mass. As electric current flow out from the mass, the negative charges will pile up at the outer side of the mass as in Figure 4.

Figure 5 Induced polarization of chargeable mass

Therefore the negative charges within the mass are polarized to the positive charges outside the mass. The positive charges within the mass are polarized to the negative charges outside the mass as in Figure 5.

Once the electric current is turned off, there will be an induced potential difference (voltage) within the mass (Kiberu, 2002). The two potential electrodes measure the decay of voltage. By integrating the area under voltage decay curve, the chargeability is obtained (Dahlin *et al*., 2002). 2-D geoelectrical imaging surveys were conducted at the site as shown in Figure 6.

3.0 MATERIALS & METHODS

3.1 Location of Study Area

The study area is located at Ladang 2 Faculty of Agriculture Universiti Putra Malaysia, Jalan Keledang, 43400 Serdang, Selangor, Malaysia with Utm coordinates 333050.6 N, 800253.2 E, and 332746.2 N, 800637.1 E. Soil in this area has developed over rocks of three formations, namely Kenny Hill, Kajang and Kuala Lumpur Formation. Kenny Hill Formation, which is of Permo-Carboniferous age is composed of quartzite and phyllite. Kajang Formation is composed of schist with minor intercalation of limestone and phyllite, whereas Kuala Lumpur Formation is composed of lime- stone with minor intercalation of phyllite (Yin, 1976 as cited in Darus, 1979). Details of the rocks are given in Table 1:

Figure 6 Location of geoelectrical imaging survey lines at Ladang 2 UPM

Table 1 Classification of parent rocks in UPM (Yin, 1976 as cited in Darus, 1979)

Age	Formation	Lithology
Permo-Carboniferous	Kenny Hill	Quartzite and phyllite
Middle-Upper Silurian	Kajang	Schist with minor intercalation of limestone and phyllite
Middle-Upper Silurian	K.L.	Limestone with minor intercalation of phyllite

3.2 Methodology

2-D geoelectrical imaging surveys were conducted at the site. In this survey, 61 electrodes were arranged in each line. There were 3 horizontal lines with 5 m spacing and 2 vertical lines with 3.8 m spacing. In ABEM SAS4000 system, the ABEM Terrameter and Lund electrode selector were used to select the relevant 4 active electrodes for each measurement of resistivity data. Schlumberger (Wenner-Schlumberger) array was used because it is moderately sensitive to the horizontal and vertical

structures. Furthermore, the Schlumberger array has the highest median depth of investigation (Loke, 2000). Using the same array, the ABEM SAS4000 system was set to induced polarization mode. The maximum current for the resistivity and induced polarization mode was 10 mA and 200 mA respectively. The electrical resistivity result was compared to the well lithology.

4.0 RESULTS & DISCUSSION

Electrical survey for line 1 has been arranged so that the well at Ladang 2 UPM will be the center of the line. The well diameter is 203.2 mm and constructed with open borehole end. The total length of well is 54 m. Location of the well in line 1 is given in Figure 7. During the well construction, soil sample was collected for every 3 m depth. The well lithology is given in Table 2. From the well lithology, it is observed that subsurface geological formation mostly dominated by schist (mud) in the upper layer. Meanwhile quartzite formation is dominating in the lower layer.

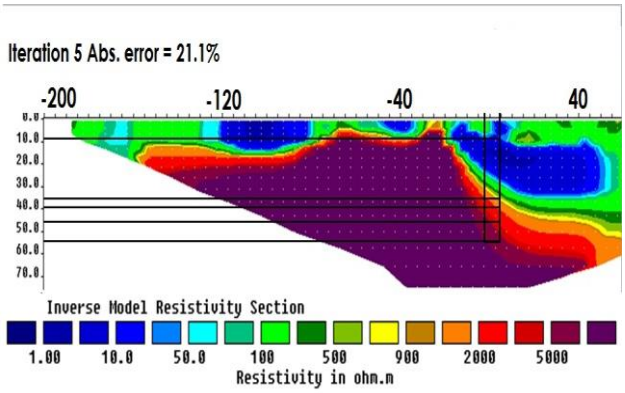

Figure 7 Well location at line 1

Table 2 Details of well lithology

Depth (m)	Geological formation
0 – 9	Top soil
9 – 36	Schist/ mud (clay + silt)
36 – 39	Conglomerate (sedimentary rocks)
39 – 46	Quartzite (metasedimentary rocks)
46 – 47	Schist/ mud (clay + silt)
47 – 54	Quartzite (metasedimentary rocks)

During the drilling process, groundwater was found at depth of 36m below ground level. Soil sample that was collected at this depth has been identified as conglomerate. Thus, the groundwater may be accumulated in a fractured aquifer. Electrical resistivity value of different geological formation was identified by comparing the 2D image of resistivity to the well lithology as illustrated in Figure 8. The electrical resistivity value for each geological formation is given in Table 3. Quartzite formation that has electrical resistivity value of 5000 to 7000 Ωm is classified as solid rock. Meanwhile quartzite formation that has electrical resistivity value range below 5000 Ωm may be fractured. It is supported by observation during the well construction where there is schist (mud) in between the quartzite formation (Table 2). This may indicate that there is fracture within quartzite formation that has electrical value below 5000 Ωm which is filled with groundwater and schist (mud).

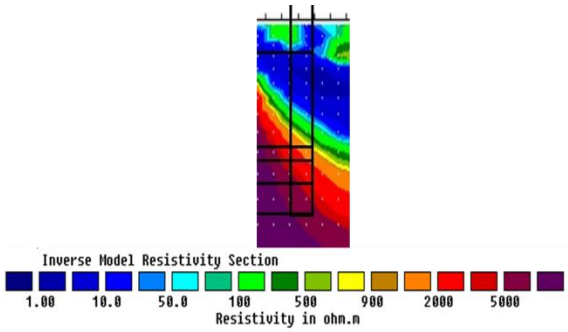

Figure 8 Electrical resistivity distribution within well

Table 3 Electrical resistivity value for geological formation

Geological formation	Electrical resistivity value (Ωm)
Top soil	0 - 300
Schist/ mud (clay + silt)	0 - 2000
Conglomerate (sedimentary rocks)	1000 - 4000
Quartzite (metasedimentary rocks)	4000 - 5000
Schist/ mud (clay + silt)	
Quartzite (metasedimentary rocks)	5000 - 7000

The electrical survey results are presented in term of inverse model of resistivity and chargeability in Figure 9 – Figure 13. The heterogeneity of geological formation can be observed in the inversed model resistivity section. There are several stripes of different electrical resistivity value ranged from 700 to 2000 Ωm above the solid rocks. By referring to the Table 3, conglomerate and fractured quartzite have electrical resistivity value ranged from 1000 t0 4000 Ωm. Therefore conglomerate and fractured quartzite mostly lied above the solid rocks.

In order to verify groundwater occurrence in the fractured area, induced polarization measurement have been conducted right after the resistivity measurement during the electrical survey. Induced polarization is measured in term of chargeability. Advantage of induced polarization is ability to distinguish groundwater from water in clayey soil.

High porosity and high groundwater conductivity reduce the chargeability value (Juanah *et al*., 2012). However the conductivity of water distributed within the soil pore is also increased by ionization and surface conductance of clay. The conductivity of fresh water and water in clay (Roy, 2014) is given in Table 4. The chargeability of high clay content is lower compared to the chargeability of high water content. Therefore it is inferred that chargeability of groundwater value is within 1msec to 2 msec; whereas below than that, it may be due to water interaction in clayey soil.

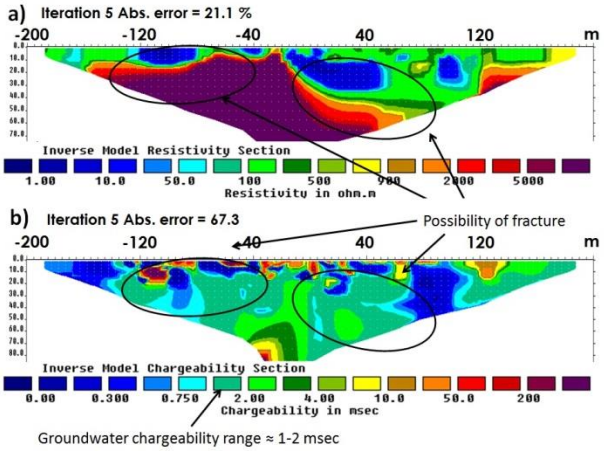

Figure 9 Location of possible fractured areas for line 1 based on a) electrical resistivity value and pattern in inversed model resistivity section and b) chargeability value in inversed model chargeability section

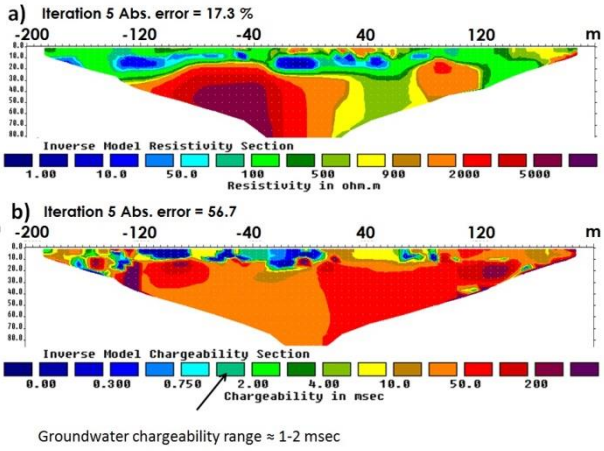

Figure 10 Location of possible fractured areas for line 2 based on a) electrical resistivity value and pattern in inversed model resistivity section and b) chargeability value in inversed model chargeability section

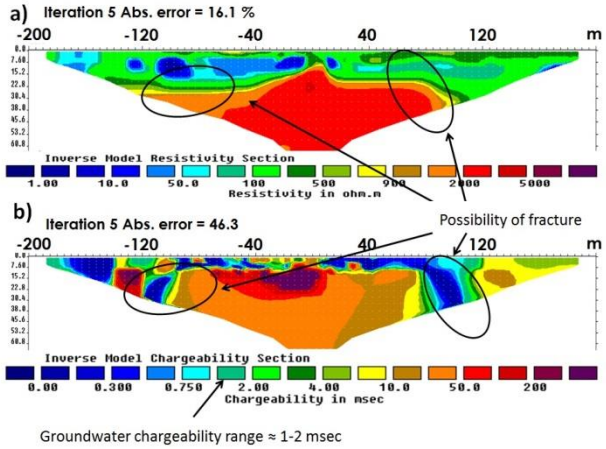

Figure 11 Location of possible fractured areas for line 3 based on a) electrical resistivity value and pattern in inversed model resistivity section and b) chargeability value in inversed model chargeability section

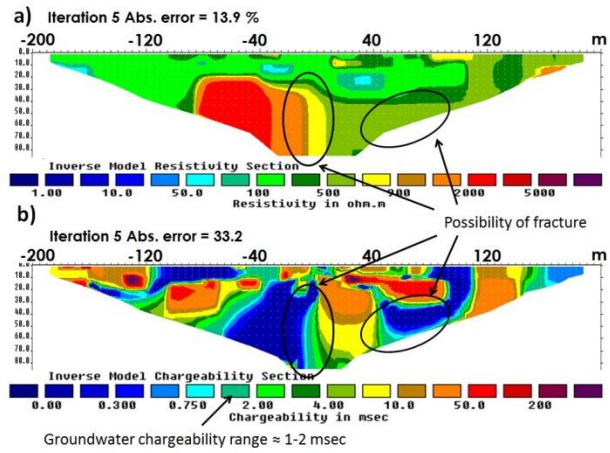

Figure 12 Location of possible fractured areas for line 4 based on a) electrical resistivity value and pattern in inversed model resistivity section and b) chargeability value in inversed model chargeability section

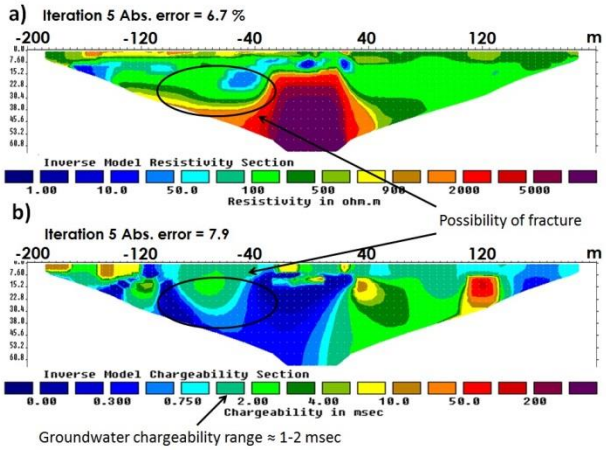

Figure 13 Location of possible fractured areas for line 5 based on a) electrical resistivity value and pattern in inversed model resistivity section and b) chargeability value in inversed model chargeability section

Table 4 Electrical conductivity for earth material (Roy, 2014)

Common earth materials of present interest	Electrical conductivity (mho/metre)
Fresh water	10^{-4} to 3 x 10^{-2}
Salt water	4
Sand (dry)	10^{-7} to 10^{-3}
Sand (saturated with water)	10^{-4} to 10^{-2}
Silt (saturated with water)	10^{-3} to 10^{-2}
Clay (saturated with water)	10^{-1} to 1
Shale	10^{-1}

Most areas that have electrical resistivity value from 700 to 2000 Ωm are overlapped with low chargeability ranged from 1 msec to 2 msec which indicate the groundwater occurrence. Therefore area that has electrical resistivity value within 700 to 2000 Ωm and overlapped with low chargeability value within 1 msec to 2 msec may be fractured. The potential fractured areas are circled in the Figure 9 – Figure 13.

5.0 CONCLUSION

The aquifer within Ladang 2 UPM has been identified as a fractured aquifer. Induced polarization analysis can reduce the ambiguities in the resistivity data. Induced polarization is able to distinguish between clay and groundwater. Combination of resistivity and induced polarization data can identify the possible fractured areas.

Acknowledgement

We are grateful to all the staffs, final year students department of biological and agricultural engineering including staffs at Ladang 2 UPM that have assisted in conducting this study.

References

[1] Anomohanran, O. 2015. Geoelectrical Evaluation of Groundwater Occurrence in Anwai, Delta State, Nigeria. 5(4): 120-127.

[2] Asfahani, J. 2007. Geoelectrical Investigation for Characterizing the Hydrogeological Conditions in Semi-Arid Region in Khanasser Valley, Syria. *Journal of Arid Environments*. 68(1): 31-52. doi:10.1016/j.jaridenv.2006.03.028.

[3] Boucher, M., Favreau, G., Descloitres, M., Vouillamoz, J. M., Massuel, S., Nazoumou, Y., Legchenko, A. 2009. Contribution of Geophysical Surveys to Groundwater Modelling of a Porous Aquifer in Semiarid Niger: An Overview. *Comptes Rendus-Geoscience*. 341(10-11): 800-809. doi:10.1016/j.crte.2009.07.008.

[4] Dahlin, T., Leroux, V., & Nissen, J. 2002. Measuring Techniques in Induced Polarisation Imaging. *Journal of Applied Geophysics*. 50(3): 279-298. doi:10.1016/S0926-9851(02)00148-9.

[5] Darus, A. 1979. Mineralogy and Genesis of Soils in Uuiversiti Pertanian Malaysia , Serdang, Selangor. 2(2): 141-148.

[6] Griffiths, D., & Barker, R. 1993. Two-dimensional Resistivity Imaging and Modelling in Areas of Complex Geology. *Journal of Applied Geophysics*. 29(3-4): 211-226. doi:10.1016/0926-9851(93)90005-J.

[7] Juanah, M. S. E., Ibrahim, S., Sulaiman, W. N. A., & Latif, P. A. 2012. Groundwater Resources Assessment Using Integrated Geophysical Techniques in the Southwestern Region of Peninsular Malaysia. *Arabian Journal of Geosciences*. 6(11): 4129-4144. doi:10.1007/s12517-012-0700-9.

[8] Kiberu, J. 2002. Induced Polarization and Resistivity Measurements on a Suite of Near Surface Soil Samples and Their Empirical Relationship to Selected Measured Engineering. Interntional Institute for Geo-Information Science and Earth Observation Enschede, The Netherlands. Retrieved from http://scholar.google.com/scholar?hl=en&btnG=Search&q=intitle:Induced+Polarization+and+Resistivity+measurements+on+a+suite+of+near+surface+soil+samples+and+their+empirical+relationship+to+selected+measured+engineering+parameters#0.

[9] Loke, M. H. 1995. Least-squares Deconvolution of Apparent Resistivity Pseudosections. *Geophysics*. 60(6): 1682. doi:10.1190/1.1443900.

[10] Loke, M. H. 2000. Electrical Imaging Surveys for Environmental and Engineering Studies. A Practical Guide to 2-D and 3-D surveys, (1999), 59. Retrieved from http://www.georentals.co.uk/Lokenote.pdf.

[11] Roy, K. K. 2014. *Recent Trends in Modelling of Environmental Contaminants*. doi:10.1007/978-81-322-1783-1.